Pliocene reversal of late Neogene aridification

J. M. Kale Sniderman[a,1], Jon D. Woodhead[a], John Hellstrom[a], Gregory J. Jordan[b], Russell N. Drysdale[c,d], Jonathan J. Tyler[e], and Nicholas Porch[f]

[a]School of Earth Sciences, University of Melbourne, Parkville, VIC 3010, Australia; [b]School of Biological Sciences, University of Tasmania, Private Bag 55, Hobart, TAS 7001, Australia; [c]School of Geography, University of Melbourne, Parkville, VIC 3010, Australia; [d]Environnements, Dynamiques et Territoires de la Montagne, UMR CNRS, Université de Savoie-Mont Blanc, 73376 Le Bourget du Lac, France; [e]Department of Earth Sciences, University of Adelaide, Adelaide, SA 5001, Australia; and [f]School of Life and Environmental Sciences, Deakin University, Burwood, VIC, 3125, Australia

The Pliocene epoch (5.3–2.6 Ma) represents the most recent geological interval in which global temperatures were several degrees warmer than today and is therefore considered our best analog for a future anthropogenic greenhouse world. However, our understanding of Pliocene climates is limited by poor age control on existing terrestrial climate archives, especially in the Southern Hemisphere, and by persistent disagreement between paleo-data and models concerning the magnitude of regional warming and/or wetting that occurred in response to increased greenhouse forcing. To address these problems, here we document the evolution of Southern Hemisphere hydroclimate from the latest Miocene to the middle Pliocene using radiometrically-dated fossil pollen records preserved in speleothems from semiarid southern Australia. These data reveal an abrupt onset of warm and wet climates early within the Pliocene, driving complete biome turnover. Pliocene warmth thus clearly represents a discrete interval which reversed a long-term trend of late Neogene cooling and aridification, rather than being simply the most recent period of greater-than-modern warmth within a continuously cooling trajectory. These findings demonstrate the importance of high-resolution chronologies to accompany paleoclimate data and also highlight the question of what initiated the sustained interval of Pliocene warmth.

paleoclimate | pollen | speleothems | aridification | Neogene

Our knowledge of Pliocene climates is based predominantly on the rich marine sediment record (1), but understanding of Pliocene climates on land remains limited because the few existing terrestrial archives tend to have poor age control and are of short duration. This deficiency is no more evident than in paleovegetation records, which are integral to modeling Pliocene climates because vegetation is both a critical indicator of regional precipitation and also makes a large contribution to planetary albedo (2, 3). Several syntheses of Pliocene vegetation have been compiled (3, 4), but their value is hampered by substantial uncertainty surrounding the synchroneity of the records. For example, vegetation syntheses have focused on the Late Pliocene (the Piacenzian Age, 3.6–2.6 Ma) because this period is considered likely to be a closer biological and geological analog for future warming than the Early Pliocene (1, 5). However, only 6 of 32 Southern Hemisphere records interpreted by Salzmann et al. (4) as documenting the nature of Late Pliocene vegetation are both based on plant fossils and can confidently be assigned to the Late Pliocene; the remaining records have such poor chronologies that their possible ages range from Late Miocene to Early Pleistocene, or the records only infer the nature of vegetation indirectly from geomorphology or vertebrate fossils (*SI Appendix*, Table S1). As a result, current understanding of the response of Southern Hemisphere vegetation to Late Pliocene climates (2–4) may conflate the climate and vegetation history of ≥5 My of the late Cenozoic (Fig. 1), an interval that is characterized by global cooling (6) and, in subtropical- to midlatitudes, increasing aridity (7–10). This uncertainty is problematic for two reasons. First, it has become clear that the peak of Pliocene warmth globally was not generally within the Late Pliocene but occurred earlier, within the Early Pliocene (11). Second, largely because of a lack of continuous and well-dated records, the relationship between the longer-

term cooling/aridification trend and Pliocene warmth remains unclear. Thus, was Pliocene warmth a discrete interruption of late Cenozoic cooling/aridification trends (6), or was the Pliocene merely an interval immediately preceding the abrupt steepening of these trends associated with the onset of extensive Northern Hemisphere glaciation (12, 13)?

To place the temporal evolution of Southern Hemisphere Pliocene vegetation and climate on a firmer chronological footing, we generated fossil pollen records from radiometrically dated speleothems (secondary cave carbonate deposits such as stalagmites and flowstones) from southern Australia. Pollen assemblages were extracted from samples collected in five caves on the Nullarbor Plain (Fig. 2 and *SI Appendix*, Fig. S1), a large (200,000 km²) karst province uplifted above sea level during the late Miocene (14). Consistent with its position in Southern Hemisphere subtropical latitudes, the Nullarbor Plain is currently semiarid, receiving mean annual precipitation (MAP) of *ca.* 180–270 mm (*SI Appendix*, Fig. S1), with a weak winter-maximum. Mean annual temperature is ∼18 °C. The vegetation is largely treeless chenopod shrubland, grading coastward into sparse, low open woodlands dominated by *Acacia* (Mimosaceae) or *Eucalyptus* (Myrtaceae). Nullarbor speleothems grew during the late Neogene (15) but negligible calcite speleothem growth occurs today. Recent development and refinement of the uranium-lead (U-Pb) chronometer has allowed high-precision geochronology of such ancient speleothem samples (15–18). Our fossil pollen record is composed of 13 polleniferous samples (out of 81 explored for pollen), the oldest dated at 5.59 ± 0.15 Ma, in the latest Miocene, and the youngest 0.41 ± 0.07 Ma, in

Significance

The warm climates of the Pliocene epoch are considered our best analog for a future anthropogenic greenhouse world. However, understanding of the nature of Pliocene climate variability and change on land is currently limited by the poor age control of most existing terrestrial climate archives. We present a radiometrically dated history of the evolution of Southern Hemisphere vegetation and hydroclimate from the latest Miocene to the middle Pliocene. These data reveal a sharp increase in precipitation in the Early Pliocene, which drove complete vegetation turnover. The development of warm, wet early Pliocene climates clearly reversed a long-term Southern Hemisphere trend of late Neogene cooling and aridification, highlighting the question of what initiated this sustained, ∼1.5-My-long interval of warmth.
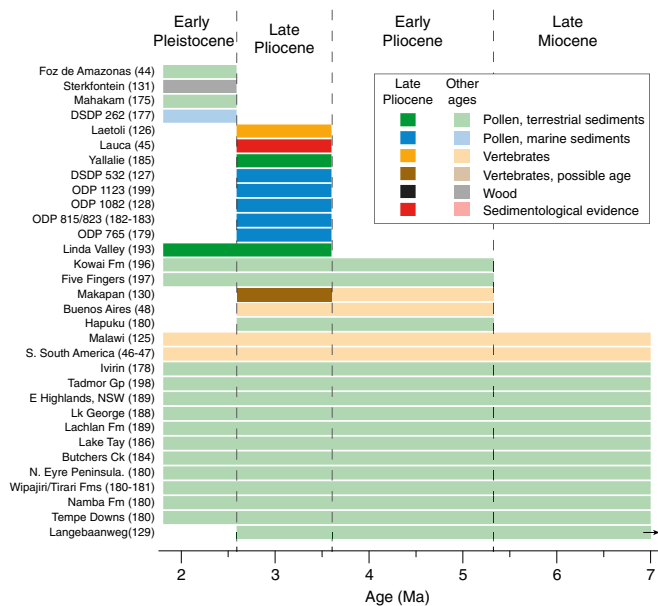
Fig. 1. Conservative estimates of the age ranges of Southern Hemisphere vegetation records accepted by Salzmann et al. (3) as indicative of Late Pliocene (Piacenzian, 2.6–3.6 Ma) terrestrial vegetation. Sample code numbers are those used by Salzmann et al. Colors represent record type (pollen, wood, vertebrate, sediment). Bold colors indicate records clearly falling within the Late Pliocene, and faint colors indicate records either falling outside of the Late Pliocene or with broader age ranges. Of the 32 records, only 6 based on plant fossil data can be confidently assigned a Late Pliocene age. For Makapan, two age estimates are provided, reflecting uncertainty whether the record can be attributed to the Pliocene as a whole or to the Late Pliocene.

the Middle Pleistocene (Table 1). Most of the samples date from the Early Pliocene (5.33–3.60 Ma).

Results and Discussion

The pollen records (Fig. 3A) indicate that, during the first *ca.* 580 ka of the record, straddling the Miocene–Pliocene boundary (between 5.59–4.97 Ma; 2σ range = 350–890 ka), the Nullarbor landscape was dominated by Gyrostemonaceae, Casuarinaceae, and *Glischrocaryon/Haloragodendron* (Haloragaceae), an assemblage of woody taxa now absent from this landscape but implying sparse shrublands or woodlands in semiarid climates (*SI Appendix,* Figs. S1B and S2 B–D). However, soon after 5 Ma, the pollen record reveals biome turnover as sparse shrublands/woodlands gave way to mesic forests of *Eucalyptus, Corymbia/Angophora* (Myrtaceae), eastern Australian type *Banksia* (Proteaceae), and *Doryanthes* (Doryanthaceae). These community types are today confined to Australia's eastern margin under moist climates with substantial summer rain (*SI Appendix,* Figs. S1B and S2, *Materials and Methods, SI Appendix, Supplementary Materials and Methods*). Pollen from the single Middle Pleistocene speleothem (Fig. 3B) is strongly dominated by chenopods, accompanied by Poaceae, Asteraceae, and Myoporeae (Scrophulariaceae), but lacking *Eucalyptus* and other Pliocene taxa altogether. This assemblage indicates that by the Middle Pleistocene, a second profound floral turnover had occurred, with vegetation similar to the modern chenopod shrubland biome of the Nullarbor Plain replacing the mesic forests (Fig. 3C).

We estimated the magnitude of hydroclimate change during latest Miocene and Early Pliocene using a probabilistic extension of the coexistence approach (19) whereby paleoclimatic inferences are based upon the distributions of the inferred living relatives of our fossil taxa. Generalized additive models (GAMs) based on vegetation survey records (*Materials and Methods*) were developed

to estimate the prevalence of the living relatives as a function of modern mean annual precipitation (MAP) (*SI Appendix,* Figs. S3 and S4). We used a Monte Carlo approach to account for propagation of uncertainties from the Gaussian 2σ error associated with each speleothem age and from the GAM-derived probability distributions of the MAP estimates (*SI Appendix, Supplementary Materials and Methods* and Fig. S5). This analysis indicates that in the latest Miocene and earliest Pliocene before *ca.* 5 Ma, MAP in the Nullarbor region was *ca.* 480 mm (320–875 mm, at the 95% confidence level; Figs. 3 and 4E) (i.e., slightly wetter than today). The absence or scarcity of pollen of the forest taxa that dominate samples later in the Pliocene (e.g., *Eucalyptus* or *Banksia*) implies that MAP was unlikely to be close to the upper end of the reconstructed interval. We therefore conclude that by the end of the Miocene, a semiarid climate had developed in the Nullarbor region that persisted for at least several hundred ka of the Early Pliocene. However, soon after 5 Ma, MAP rose rapidly (within *ca.* 100 ka, or within ≤350 ka, at the 95% confidence level) to *ca.* 1,220 mm (*ca.* 635–2,100 mm, at the 95% confidence level) and was maintained for *ca.* 1.5 My at levels two to four times higher than today.

The timing of biome turnover in the Early Pliocene Nullarbor pollen record corresponds closely to abrupt increases in sea-surface temperature (SST) apparent at low- and high-latitude sites in the Southern Hemisphere (Fig. 2). This warming is seen in Ocean Drilling Program (ODP) Site 590B in the southwest Pacific Ocean at ~5.49 Ma (Fig. 4C) and at ~5.26 Ma, in both ODP Site 763 in the eastern Indian Ocean northwest of Australia (Fig. 4D) and ODP site 1095 in the Bellingshausen Sea at the Antarctic margin (Fig. 4G). Ice-rafted debris at ODP Site 1165 in Prydz Bay declined soon afterward, at 5.04 Ma (Fig. 4F). The synchroneity of these widely separated surface temperature proxies implies that increased Nullarbor precipitation and the associated shift to more mesic, moisture-demanding vegetation were responses to a hemisphere-wide pattern of increasing temperatures during the Early Pliocene. The positive relationship between hemispheric temperatures and Nullarbor precipitation is consistent with Early Pliocene climate simulations using prescribed SSTs (20), in which atmospheric subsidence in subtropical regions was weakened markedly and convective precipitation over continents was enhanced by increased atmospheric water content. After ~3.45 Ma, the loss of the pollen record may simply be a sampling effect, but the loss does coincide closely with the timing of declining SSTs northwest of Australia at ODP 763 (Fig. 4D), increased ice-rafted debris at ODP 1165 in Prydz Bay (Fig. 4F), and major expansion of the western (21) and eastern (22) Antarctic ice sheets, suggesting that Southern Hemisphere low- to midlatitude SSTs and precipitation were linked to circum-Antarctic cooling.
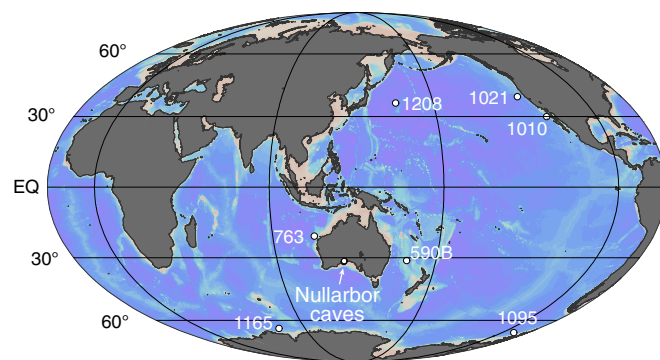

Fig. 2. Locality map showing Nullarbor caves in southern Australia and sites mentioned in the text. The map was produced using Ocean Data View (odv.awi.de).

Table 1. Age and pollen yield of Nullarbor speleothems

Sample	Age, Ma (±2σ)	Mass dissolved, g	Pollen count	Pollen grains g^{-1}
2121-1	0.41 ± 0.07	215.48	401	1.9
645-15	3.47 ± 0.13	139.06	547	3.9
370-3	3.62 ± 0.14	311.68	105	0.3
370-1	3.63 ± 0.17	221.69	35	0.2
370-5	3.76 ± 0.12	198.75	221	1.1
645-13	4.14 ± 0.11	202.77	166	0.8
370-11	4.15 ± 0.12	302.09	256	0.8
2200-12.4	4.16 ± 0.12	57.8	389	6.7
2200-2	4.20 ± 0.14	68.47	279	4.1
483-9	4.89 ± 0.12	181.89	91	0.5
370-16	4.97 ± 0.12	760.1	60	0.1
370-17	5.34 ± 0.12	247.49	113	0.5
370-19	5.59 ± 0.15	240.83	152	0.6
		$\sum = 3{,}148$	$\sum = 2{,}815$	$\bar{x} = 1.7$

The concurrent Early Pliocene warming and wetting demonstrated here suggests that Pliocene warmth in the Southern Hemisphere took the form of a discrete and sustained (≥1.5 My) interval that reversed late Neogene cooling and drying trends. Warming across the Late Miocene–Early Pliocene transition has previously been inferred from mid-high latitude Southern Hemisphere planktonic δ^{18}O records (23) and marine faunal assemblages (24, 25), whereas apparently correlative increases in precipitation have been inferred from Australian sediment and pollen records (26, 27), but difficulties in dating and quantifying these changes in terms of precipitation (28, 29) have hindered the development of a coherent model of these changes' timing, duration, and spatial extent. This reversal was not confined to the Southern Hemisphere. Intervals of warming, or at least interruptions to cooling, involving positive SST changes of 4–6 °C, sustained for at least ~1 My, were initiated in the northern Pacific Ocean at ~5.76 Ma (ODP Sites 1208, 1010, and 1021; Fig. 4A), apparently slightly earlier than the onset of warming in the southwest Pacific (ODP Site 590B; Fig. 4C) and spreading to the southern Indian Ocean, Australia, and the Antarctic by ~5.3 Ma (Fig. 4 C–G).

The mechanisms that drove the abrupt increase in Nullarbor precipitation and Southern Hemisphere sea surface temperatures are unknown. An obvious proximate explanation is provided by changes in atmospheric pCO$_2$, but understanding of pCO$_2$ history across the Miocene–Pliocene boundary is currently limited by the low resolution and potentially inconsistent oceanographic biases of available reconstructions (30). Hemisphere-wide Early Pliocene warming is consistent with an apparent upward step in alkenone-based atmospheric pCO$_2$ reconstructions from the latest Miocene to the Early Pliocene (31, 32) (Fig. 4H). However, recent alkenone-based pCO$_2$ reconstructions recovered from a single marine core (30) (Fig. 4H) provide little explanation for the temperature change from the late Miocene to Late Pliocene, although their temporal resolution over the latest Miocene/earliest Pliocene is very low. Until more detailed pCO$_2$ reconstructions are available for this interval, two scenarios remain viable: Early Pliocene warming was a first-order positive response to increased greenhouse forcing (2); or, minor fluctuations in Late Miocene–Pliocene pCO$_2$ alone cannot explain substantial climate changes over this interval, which instead may have been caused by changes in ocean circulation, perhaps associated with progressive changes in heat transport across oceanic gateways (33, 34).

Understanding of the causes of Pliocene warmth has been inhibited by confusion and uncertainty about the temporal evolution of late Neogene climate. The Pliocene is frequently associated with the notion that an extended (240-ka-long) "warm period" occurred near the end of the Epoch between ca. 3.025–3.264 Ma (35), but the warmth of this period is distinctive only when looking at the Pliocene from a Pleistocene perspective, and it is clear from the composite benthic δ^{18}O record (Fig. 4B) and from global SST records (11) that this period was relatively cool/glaciated, in the context of the Pliocene as a whole. Although a compilation of Mg/Ca- and alkenone-based SST records (11) has demonstrated that, globally, Pliocene SSTs peaked between ~4.0–4.5 Ma, no extended interval of substantial warming/deglaciation interrupts the remarkably stable late Neogene benthic δ^{18}O cooling/glaciation trend that established by ~10 Ma (13, 36) (Fig. 4B). The difference between the SST and benthic δ^{18}O signals is perhaps not surprising, if the latter integrates varying Northern and Southern Hemisphere bottom water temperature histories and perhaps regional changes in moisture supply to ice sheets (13). However, the difference emphasizes that the benthic δ^{18}O record has not been an informative guide to the temporal evolution of late Neogene surface temperature and hydroclimate. On the basis of highly smoothed interpretations of the north Pacific Ocean ODP Sites 1208, 1010, and 1021 SST records, LaRiviere et al. (12) argued that Pliocene climates, however "warm," were actually the youngest portion of an essentially uninterrupted trajectory of late Neogene cooling. However, by ~5.7 Ma, all of these sites temporarily reversed their cooling trajectories (Fig. 4A), ultimately achieving temperatures that had not been experienced since ~7–8 Ma. Thus, in both the Southern and Northern Hemispheres, Pliocene warmth was focused in the Early Pliocene and represented a reversal of late Miocene cooling trends. This reversal implies that there was a temporary change in the nature of the boundary conditions that were driving late Neogene refrigeration (6).

Efforts to understand Pliocene warmth are currently focused intensely on data-model syntheses within the Late Pliocene (2, 5), on the assumption that existing knowledge of vegetation at this time is internally consistent and representative of the vegetation response to Pliocene greenhouse climates. However, incorrect assignment of poorly dated Late Miocene, Early Pliocene, or Early Pleistocene vegetation records to the Late Pliocene (Fig. 1) may lead to the impression that the cool and potentially dry Late Pliocene (relative to the Early Pliocene) was wetter and warmer, or had more spatially diverse vegetation and climate, than was actually the case. This impression is particularly concerning if characteristically warm (and in subtropical regions, wet) Pliocene climates were confined to a relatively brief (≤1–2 My) window within the late Neogene and were distinctly warmer and wetter than most of the past ~7–8 My. If the globally warmest interval of the Pliocene thus represents a relatively small "target," excellent age control is needed to avoid conflating cooler and warmer intervals. Persistent paleovegetation data-model mismatches associated with simulations of Late Pliocene climate have been interpreted (4, 5) as resulting mainly from an inability to distinguish warm and cold orbital stages in the vegetation records. One proposed

Fig. 3. Late Miocene, Pliocene, and Middle Pleistocene vegetation change in semiarid southern Australia. Monte Carlo simulations of the late Miocene–Pliocene (*A*) and Middle Pleistocene (*B*) U-Pb–dated Nullarbor speleothem pollen record, accounting for Gaussian uncertainties in speleothem ages and in pollen percentage counts, and of the Nullarbor mean annual precipitation reconstruction derived from the pollen assemblages. The chenopod-dominated Middle Pleistocene assemblage is very similar to the composition of Late Pleistocene and Holocene pollen records (*C*) from Nullarbor cave/doline infills (43), confirming that the speleothem pollen assemblages register the surrounding vegetation in comparable ways to conventional fossil pollen records. U/Pb ages ±2σ errors are shown for 13 polleniferous samples (color-coded by cave), against the backdrop of other Nullarbor speleothems investigated for pollen (gray).

solution (5) is to focus modeling effort on a single, warm interglacial at 3.205 Ma and to limit vegetation comparisons to records in which this interglacial can be identified. Unfortunately, this approach would currently reduce the number of useful Southern Hemisphere vegetation records to four, three of which

Fig. 4. Nullarbor mean annual precipitation reconstruction and proxies for Southern Hemisphere and northern Pacific Ocean sea surface temperatures. (*A*) Alkenone-derived SST records from north Pacific Ocean ODP sites 1208, 1010, and 1021 (12); warm intervals are indicated by pink shading (for locations, see Fig. 2); note the separate time axis compared with *B–H*. (*B*) Benthic foraminifera δ^{18}O record (44) with 10-ka smoothing (dark purple line), change points at 6.14 and 3.45 Ma. (*C*) Mg/Ca-derived SSTs, ODP Site 590B, south-western Pacific (34); change points are at 5.49 and 4.35 Ma. (*D*) Mg/Ca-derived SSTs, ODP Site 763, north-eastern Indian Ocean (33); the warm interval is defined by change points at 5.26 and 3.44 Ma, indicated by yellow shading. (*E*) Monte Carlo simulation of Nullarbor late Miocene–Pliocene mean annual precipitation. (*F*) Ice-rafted debris (>125 μm), ODP Site 1165, Prydz Bay (45); change points are at 5.22, 5.04, 3.22, and 2.95 Ma. (*G*) Opal deposition rate, ODP Site 1095, Bellinghausen Sea, interpreted at this site as a proxy for open water, hence SST (46); change points are at 5.27 and 3.02 Ma. (*H*) Proxy reconstructions of atmospheric *p*CO₂, derived from alkenones [turquoise (31) and yellow (32) shading, green circles with error bars (30)], and from δ^{11}B [gray shading (47)]. Red horizontal lines are significant change points in the mean for *B–D* and *F* and *G*. Shaded boxes indicate the duration of intervals of warming.

are marine sediment records that provide highly spatially averaged vegetation histories (*SI Appendix*). Although vegetation differences between the coldest and warmest parts of Late Pliocene orbital cycles may have been significant, especially at high latitudes, a lower order explanation for some of the data-model mismatch, at least in the Southern Hemisphere, may simply be misinterpretation of the age of many poorly dated late Neogene vegetation records.

The use of the U-Pb chronometer to date pre-Pleistocene speleothems is still in its infancy (17), but Pliocene speleothems are already recorded from South Africa (37) and Israel (38). The development of U-Pb–dated speleothem pollen records thus has the potential to accurately document the temporal evolution of Pliocene vegetation and terrestrial climate in many regions, while also providing a new basis for regional correlation of poorly dated terrestrial records.

Materials and Methods

Pollen Analyses. Fossil pollen typically is present in speleothems in very low concentrations, so pollen-processing techniques were developed both to minimize contamination by modern pollen and to maximize recovery. In addition, processing methods had to accommodate the highly variable organic matter content of the speleothems, and to remove a clay- to fine silt-sized mineral fraction present in many samples, which was resistant to cold hydrofluoric acid and which can become electrostatically attracted to pollen grains, inhibiting their identification. After cutting samples with a diamond rock saw, all subsequent physical and chemical processes were carried out within a high efficiency particulate air-filtered exhausting clean air cabinet in an International Organization for Standardization (ISO) Class 7 clean room (*SI Appendix*). Where possible, >100 pollen grains were counted from each sample. To achieve this sum, in some cases, several aliquots of speleothem were dissolved, up to 760 g, and in most cases, the entire acid- and alkali-resistant residue was examined. Pollen was counted under compound light microscopy at 640× and 1,600× magnification on a Zeiss Axiolab A1 with N-Achroplan objectives and photographed on a Zeiss Axioscope A1 compound microscope with EC Plan-Neofluar objectives. All identified pollen types were included in pollen sums (Dataset S1).

Paleoprecipitation Estimates. We estimated mean annual precipitation for the 13 pollen assemblages, based on a probabilistic extension of the mutual climatic range approach. We interpreted the affinities of the Nullarbor fossil pollen types to extant plant taxa or clades and then gathered modern occurrence data for these taxa or clades, drawing on publically accessible online databases of plant occurrence data, for Australia, New Zealand, and globally. We restricted our data search to systematic survey data, in which multiple species records from a single site include (at least nominally) all plant taxa that were present at the time of survey. From the resulting dataset of plant surveys, mean annual precipitation was reconstructed based on probability

distribution functions inferred using generalized additive modeling. For each clade, we created a GAM with mean annual precipitation as the independent variable and presence/absence of the clade as the dependent variable, assuming a binomial distribution and a cubic regression spline. To calculate the joint probability function for each of the 13 Nullarbor fossil pollen samples relative to mean annual precipitation we multiplied the individual relative probability functions of each clade present within that pollen sample and then scaled the resulting function so that the cumulative total was 1 (*SI Appendix*).

Geochronology. The analytical methods used in this study follow closely those published previously by Woodhead et al. (15, 39) (also see *SI Appendix*).

Iterative Age Modeling. Each of our 13 pollen samples is derived from a separate speleothem. Because some samples had overlapping 2σ age uncertainties, we modeled the probabilities of the samples' true chronological sequence using a Monte Carlo procedure, iteratively sampling the Gaussian age distributions of each speleothem, and repeating the process 100,000 times to develop a composite probability distribution, which we summarize in terms of the distribution's median, lower and upper 1- and 2σ values. We simultaneously undertook a Monte Carlo procedure to account for binomial probability distribution of observed pollen percentages. For both Monte Carlo simulations, the resulting probability cloud was binned into a 2D histogram of 500 by 500 bins. A cumulative probability curve was compiled for each time slice of the histogram that lies within 2σ of an age determination, from which y values were determined for the median and for corresponding upper- and lower-95% confidence intervals (*SI Appendix* and Dataset S1).

Time Series Analysis. We located significant change points (40) in the mean of time series using the cpt.mean function in the changepoint package (41) in R (42) (*SI Appendix*).

Evaluation of the Ages of Published Southern Hemisphere Vegetation Records. We critically reviewed the quality of the age control of all Southern Hemisphere records interpreted by Salzmann et al. (3, 4) as evidence for Late Pliocene (the Piacenzian epoch) vegetation. We assigned conservative age estimates to each record (*SI Appendix*, Table S1), defined in relation to the strength of age control (*SI Appendix*).

1. Dowsett HJ, et al. (2012) Assessing confidence in Pliocene sea surface temperatures to evaluate predictive models. *Nat Clim Chang* 2(5):365–371.
2. Haywood AM, et al. (2013) Large-scale features of Pliocene climate: Results from the Pliocene Model Intercomparison Project. *Clim Past* 9(1):191–209.
3. Salzmann U, Haywood AM, Lunt DJ, Valdes PJ, Hill DJ (2008) A new global biome reconstruction and data-model comparison for the Middle Pliocene. *Glob Ecol Biogeogr* 17(3):432–447.
4. Salzmann U, et al. (2013) Challenges in quantifying Pliocene terrestrial warming revealed by data-model discord. *Nat Clim Chang* 3(11):969–974.
5. Haywood AM, et al. (2013) On the identification of a Pliocene time slice for data-model comparison. *Philos Trans A Math Phys Eng Sci* 371(2001):20120515.
6. Zachos J, Pagani M, Sloan L, Thomas E, Billups K (2001) Trends, rhythms, and aberrations in global climate 65 Ma to present. *Science* 292(5517):686–693.
7. Cane MA, Molnar P (2001) Closing of the Indonesian seaway as a precursor to east African aridification around 3-4 million years ago. *Nature* 411(6834):157–162.
8. Martin HA (2006) Cenozoic climatic change and the development of the arid vegetation in Australia. *J Arid Environ* 66(3):533–563.
9. Cerling TE, et al. (1997) Global vegetation change through the Miocene/Pliocene boundary. *Nature* 389(6647):153–158.
10. Fauquette S, et al. (2007) Latitudinal climatic gradients in the Western European and Mediterranean regions from the Mid Miocene (c. 15 Ma) to the Mid-Pliocene (c. 3.5 Ma) as quantified from pollen data. *Deep-Time Perspectives on Climate Change: Marrying the Signal from Computer Models and Biological Proxies*, eds Williams M, Haywood AM, Gregory FJ, Schmidt DN (The Micropalaeontological Society, London), pp 481–502.
11. Fedorov AV, et al. (2013) Patterns and mechanisms of early Pliocene warmth. *Nature* 496(7443):43–49.
12. LaRiviere JP, et al. (2012) Late Miocene decoupling of oceanic warmth and atmospheric carbon dioxide forcing. *Nature* 486(7401):97–100.
13. Mudelsee M, Bickert T, Lear CH, Lohmann G (2014) Cenozoic climate changes: A review based on time series analysis of marine benthic δ18O records. *Rev Geophys* 52(3):333–374.
14. Webb JA, James JM (2006) Karst evolution of the Nullarbor Plain, Australia. *Spec Pap Geol Soc Am* 404:65–78.
15. Woodhead J, et al. (2006) U–Pb geochronology of speleothems by MC-ICPMS. *Quat Geochronol* 1:208–221.
16. Richards DA, Bottrell S, Cliff RA, Strohle K, Rowe P (1998) U–Pb dating of a speleothem of Quaternary age. *Geochim Cosmochim Acta* 62(23-24):3683–3688.
17. Woodhead J, et al. (2012) U and Pb variability in older speleothems and strategies for their chronology. *Quat Geochronol* 14:105–113.
18. Bajo P, Drysdale R, Woodhead J, Hellstrom J, Zanchetta G (2012) High-resolution U–Pb dating of an Early Pleistocene stalagmite from Corchia Cave (central Italy). *Quat Geochronol* 14:5–17.
19. Mosbrugger V, Utescher T (1997) The coexistence approach- A method for quantitative reconstructions of Tertiary terrestrial palaeoclimate data using plant fossils. *Palaeogeogr Palaeoclimatol Palaeoecol* 134(1-4):61–86.
20. Brierley CM, et al. (2009) Greatly expanded tropical warm pool and weakened Hadley circulation in the early Pliocene. *Science* 323(5922):1714–1718.
21. McKay R, et al. (2012) Antarctic and Southern Ocean influences on Late Pliocene global cooling. *Proc Natl Acad Sci USA* 109(17):6423–6428.
22. Patterson MO, et al. (2014) Orbital forcing of the East Antarctic ice sheet during the Pliocene and Early Pleistocene. *Nat Geosci* 7(11):841–847.
23. Hodell DA, Kennett JP (1986) Late Miocene-Early Pliocene stratigraphy and paleoceanography of the South Atlantic and Southwest Pacific Oceans: A synthesis. *Paleoceanography* 1(3):285–311.

EARTH, ATMOSPHERIC, AND PLANETARY SCIENCES

24. Kennett JP, Vella P (1975) Late Cenozoic planktonic foraminifera and palaeoceanography at DSDP Site 284 in the cool subtropical south Pacific. *Initial Rep Deep Sea Drill Proj* 29:769–782.
25. McGowran B, Li QY, Moss G (1997) The Cenozoic neritic record in southern Australia: The biogeohistorical framework. *Cool-Water Carbonates*, eds James NP, Clarke JAD (Society for Sedimentary Geology, Tulsa, OK).
26. Martin HA (1973) Upper Tertiary palynology in southern New South Wales. *Special Publication Geol Soci Aust* 4:35–54.
27. Benbow MC, Alley NF, Callen RA, Greenwood DR (1995) Geological history and palaeoclimate. *The Geology of South Australia: The Phanerozoic*, eds Drexel J, Preiss W (South Australia Geological Survey, Adelaide, South Australia), Vol 2, pp 208–218.
28. Kershaw AP, Martin HA, McEwan Mason JRC (1994) The Neogene: A period of transition. *History of the Australian Vegetation: Cretaceous to Recent*, ed Hill RS (Cambridge Univ Press, Cambridge, UK), pp 299–327.
29. Macphail M (2007) *Australian Palaeoclimates: Cretaceous to Tertiary – A Review of Palaeobotanical and Related Evidence to the Year 2000. CRC LEME Open File Report 151* (Cooperative Research Centre for Landscape Environments and Mineral Exploration, Bentley, Australia).
30. Zhang YG, Pagani M, Liu Z, Bohaty SM, Deconto R (2013) A 40-million-year history of atmospheric CO(2). *Philos Trans A Math Phys Eng Sci* 371(2001):20130096.
31. Pagani M, Freeman KH, Arthur MA (1999) Late Miocene atmospheric CO_2 concentrations and the expansion of C_4 grasses. *Science* 285(5429):876–879.
32. Seki O, et al. (2010) Alkenone and boron-based Pliocene pCO2 records. *Earth Planet Sci Lett* 292(1–2):201–211.
33. Karas C, Nürnberg D, Tiedemann R, Garbe-Schönberg D (2011) Pliocene Indonesian Throughflow and Leeuwin Current dynamics: Implications for Indian Ocean polar heat flux. *Paleoceanography* 26(2):PA2217.
34. Karas C, Nürnberg D, Tiedemann R, Garbe-Schönberg D (2011) Pliocene climate change of the Southwest Pacific and the impact of ocean gateways. *Earth Planet Sci Lett* 301(1-2):117–124.
35. Dowsett HJ, et al. (2013) The PRISM (Pliocene palaeoclimate) reconstruction: Time for a paradigm shift. *Philos Trans A Math Phys Eng Sci* 371(2001):20120524.
36. Lisiecki LE, Raymo ME (2005) A Pliocene-Pleistocene stack of 57 globally distributed benthic δ18O records. *Paleoceanography* 20(1):PA1003.
37. Pickering R, Kramers JD (2010) Re-appraisal of the stratigraphy and determination of new U-Pb dates for the Sterkfontein hominin site, South Africa. *J Hum Evol* 59(1): 70–86.
38. Vaks A, et al. (2013) Pliocene–Pleistocene climate of the northern margin of Saharan–Arabian Desert recorded in speleothems from the Negev Desert, Israel. *Earth Planet Sci Lett* 368:88–100.
39. Woodhead J, et al. (2010) Speleothem climate records from deep time? Exploring the potential with an example from the Permian. *Geology* 38(5):455–458.
40. Chen J, Gupta AK (2000) *Parametric Statistical Change Point Analysis* (Birkhauser, New York).
41. Killick R, Eckley I (2014) changepoint: An R package for changepoint analysis. *J Stat Softw* 58(3):1–19.
42. Team RDC (2003) *R: A Language and Environment for Statistical Computing* (Foundation for Statistical Computing, Vienna).
43. Martin HA (1973) Palynology and historical ecology of some cave excavations in the Australian Nullarbor. *Aust J Bot* 21(2):283–316.
44. Zachos JC, Dickens GR, Zeebe RE (2008) An early Cenozoic perspective on greenhouse warming and carbon-cycle dynamics. *Nature* 451(7176):279–283.
45. Passchier S (2011) Linkages between East Antarctic Ice Sheet extent and Southern Ocean temperatures based on a Pliocene high-resolution record of ice-rafted debris off Prydz Bay, East Antarctica. *Paleoceanography* 26(4):PA4204.
46. Hillenbrand CD, Ehrmann W (2005) Late Neogene to Quaternary environmental changes in the Antarctic Peninsula region: Evidence from drift sediments. *Global Planet Change* 45(1-3):165–191.
47. Bartoli G, Hönisch B, Zeebe RE (2011) Atmospheric CO2 decline during the Pliocene intensification of Northern Hemisphere glaciations. *Paleoceanography* 26(4):PA4213.